Numerical and Experimental Studies of Halo Formation Due to Mismatch in a Space-Charge Dominated Electron Beam*

D. Kehne** and M. Reiser
Laboratory for Plasma Research
University of Maryland 20742

H. Rudd
6922 Nashville Rd.
Lanham, MD 20706

Abstract

Numerical and experimental studies of emittance growth and halo formation arising from beam mismatch have been performed. A mismatched 5 keV, 44 mA electron beam distribution passes through a 36-solenoid transport channel. Past studies have verified the agreement between experiment, simulation, and theory. Past simulation results show that a halo is responsible for emittance growth that results from the mismatch. Now simulation is used to find correlation between the initial distribution and the halo.

I. INTRODUCTION

Intense beams needed for applications such as FELs, electron-positron colliders, and Heavy Ion Inertial Fusion must maintain minimal emittance and size throughout the acceleration and transport region. Studies show that emittance growth arising from beam mismatch manifests itself in the form of a halo[1,2,3]. The halo is responsible for most of the emittance growth predicted by theory. Studies of multiple beams at the University of Maryland[3,4] provide a useful tool to explore halo formation.

II. BACKGROUND THEORY

Formulas predicting emittance growth due to conversion of free energy have been developed[5,6] and tested[3,4]. Theory predicts rms emittance growth of

$$\frac{\varepsilon_f}{\varepsilon_i}=\frac{a_f}{a_i}\left[1+\frac{\sigma_o^2}{\sigma_i^2}\left(\frac{a_f^2}{a_i^2}-1\right)\right]^{1/2} \tag{1}$$

where σ_i and σ_o are the phase advances per cell with and without space charge, a_i and a_f are the 2×rms radii of the equivalent initial stationary beam and the equivalent final stationary beam. For period length S, σ_i can be calculated as $\sigma_i^2/S^2 = \sigma_o^2/S^2 - K/a_i^2$ where $K=2(I/I_o)/(\beta\gamma)^3$, I is the beam current, $I_o=1.7\times10^4$ A, β and γ are the usual relativistic factors and a_f/a_i can be found using

$$\frac{a_f^2}{a_i^2}-1-\left(1-\frac{\sigma_i^2}{\sigma_o^2}\right)\ln\frac{a_f}{a_i}=h. \tag{2}$$

For nonuniform charge distributions, the value of h is[5]

$$h=h_s=\frac{1}{4}\left(1-\frac{\sigma_i^2}{\sigma_o^2}\right)\frac{U}{w_o}, \tag{3}$$

where U/w_o is a dimensionless parameter depending only on the geometry of the distribution. For mismatched beams[5],

$$h_m=\frac{1}{2}\frac{\sigma_i^2}{\sigma_o^2}\left(\frac{a_i^2}{a_o^2}-1\right)-\frac{1}{2}\left(1-\frac{a_o^2}{a_i^2}\right)+\left(1-\frac{\sigma_i^2}{\sigma_o^2}\right)\ln\frac{a_i}{a_o}, \tag{4}$$

where a_o is the effective radius of the mismatched beam at the beginning of the channel. A waist is assumed here. In the presence of both effects, h_s and h_m add.

III. EXPERIMENTAL SETUP

The Electron Beam Transport Facility has been used to study the dynamics of multiple beam merging[3,4,7]. A 5-beamlet distribution of 44 mA and 5 keV is created by masking a 240 mA e⁻ beam. The 4×rms-emittance of the 5-beamlet distribution is estimated at 65π mm-mrad. This beam passes through 2 solenoids which mismatch the configuration to the 36 solenoid periodic (S=13.6 cm) channel that follows. The mismatch ratio(a_o/a_i) is 0.5. The values of σ_o and σ_i are 77° and 23° respectively and U/w_o was found to be 0.2656. A slit/pinhole device measures the emittance of the beam at the end of the channel. A movable phosphor screen is used to record pictures along the entire channel. Simulations were performed with the PIC code SHIFTXY described elsewhere[2]. In this paper, parameter z is defined as the distance from the aperture plate and N is the number of periods from the channel entrance.

IV. RESULTS

The two expected sources of emittance growth in this experiment are space-charge nonuniformity and mismatch. Previous studies[4] show that charge redistribution of the 5-beamlets causes the rms-emittance to grow by a factor of 1.5. This occurs in a quarter of a plasma wavelength, in agreement with theory, corresponding to a point midway between the two matching lenses. As the beam passes into the channel, the rms-emittance grows again as the free energy of the mismatch converts to kinetic energy, levelling off after 12 channel periods. A plot of emittance growth versus period number obtained from the computer simulation is shown in Fig. 1. Experimental pictures and simulated data revealed that, unlike for a matched beam, a halo forms around a

*Work supported by the U.S. DOE
**Presently employed at CEBAF

thermalized core. Elimnation of this halo via simulation resulted in a beam with no emittance growth past that due to the charge redistribution.

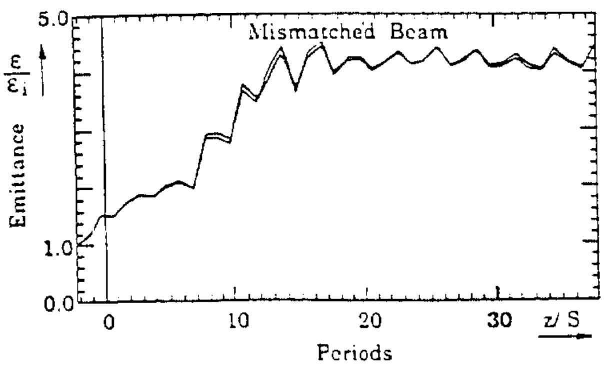

Fig. 1. Emittance growth plotted versus period number.

In this case, rms quantities do not reveal the details of the particle dynamics. Since the simulations are reliable, they are used to track the halo particles back to the initial phase space. The halo must first be defined. The x-y and x'-y' phase spaces of the beam at the beginning(N=-2.25) and end of the channel(N=36.3) are shown in Fig. 3a-d. The halo is clearly evident at N=36.3. We define halo particles somewhat arbitrarily as either having radial postion r greater than $r_{max}/2$ or slope r' greater than $r'_{max}/2$. By this definition, the halo is found to comprise 17% of the total beam current[3].

There is some question as to whether particles are swapped between the core and the halo. Comparision of halo particles at locations N=14, 22, 30, and 36 and shows that 80-90% recurrence of halo particles. The remnant mismatch causes the halo conditions to vary between these points and makes determination of the core/halo boundary difficult. The percentage of recurring halo particles could be much higher.

In order to determine correlations between halo particles and their position in the initial phase space, halo particles at N=36.3 are tracked back to the aperture plate. The problem is simplified by only considering particles originating from the inner beamlet and one outer beamlet. Phase space plots of core particles at N=36.3 originating from the inner beamlet are shown in Fig. 3e and f and from the outer beamlet in Fig 3g and h. The same plots of halo particles are shown in Figs. 3i-l. Note that the core of the outer beamlet is centered in the beamline while the halo is not. Substantial structure is evident in the halos of the beamlets while both cores are essentially thermalized. This inequity between the halo and core thermalization rates has also been noted by Wangler [2].

Phase space plots of particles in the initial distribution that will eventually enter the core are shown in Fig. 4m and n and the halo plots are in Figs. 3o and p. Several observations can be made from these plots. First, the inner beamlet contributes particles uniformly from its x-y phase space. Second, the outer beamlet contributes to the halo predominantly from the outer edge away from the beam center. Though core particles from the outer beamlet derive mostly from the edge facing the inner beamlet, many still lie on the outer edge. Fig. 3n shows that certain regions of the x-x' phase space are excluded from the core entirely. These are particles with high velocities and high values of x.

The reason that particles are determined by both initial positon and velocity is simple. The electrostatic field set up by the 5-beamlet distribution exerts a force to either speed up or slow down each particle. This field is highest at the outer edge of the outer beamlet and lowest at the inner edge of the outer beamlet (and at the center of the center beamlet). Many halo particles come from the portion of the initial distribution that either gets the largest boost from the self-field or have large kinetic energy(KE) and are unaffected by the E-field. Likewise, core particles are genrerally determined by low KE, low E-field, or high velocity-cancelling E-field. This can be quantified by calculating the average KE of the various particles at z=0(the initial distribution) and after z=1 cm of propagation under the influence of the E-field. Table I summarizes these numbers. Despite these numbers, there are substantial numbers of particles that seem to gain energy later in the transport and hence enter the halo.

Table I. KE of core and halo particles at z = 0 cm.

	Core Particles		Halo Particles	
KE	inner	outer	inner	outer
(z=0)	0.43 eV	0.40 eV	0.63 eV	0.74 eV
(z=1 cm)	0.43 eV	0.40 eV	0.66 eV	0.79 eV

V. CONCLUSION

The analysis of the simulation data showing halo formation during the transport of a mismatched beam has led to several expected conclusions. First, most of the energy associated with the mismatch goes into the halo. Second, the beam core thermalizes much faster than the surrounding halo. Also, many of the particles that form the halo are determined by their position in the initial distribution. Though halo particles are found to be those particles of highest kinetic and potential energies, it is clear that subsequent dynamics play a part in the core/halo determination.

VI. REFERENCES

[1]O.A. Anderson and L. Soroka, Proc. of 1987 Part. Accel. Conf., Washington, DC, IEEE Cat. No. 87CH2387-9 1043, (1987).

[2]T. Wangler, Proc. of Symposium on High Brightness Beams for Advanced Accel. Appl., AIP Conference Proc. No. 253, 21 (1991).

[3]D. Kehne, M. Reiser, and H. Rudd, Proc. of Symposium on High Brightness Beams for Advanced Accel. Appl., AIP Conference Proc. No. 253, 47 (1991).

[4]I. Haber, D. Kehne, M. Reiser, and H. Rudd, Phys. Rev. A, **44** (6), 5194 (1991).

[5]M. Reiser, J. Appl. Phys. 70 (4), 1919 (1991).

[6]T. Wangler, K. Crandall, R. Mills, and M. Reiser, IEEE Trans. Nucl. Sci., NS-32 2196 (1985).

[7]D. Kehne, PhD Dissertation, Electrical Engineering Dept., Unviversity of Maryland, College Park, MD (1992).

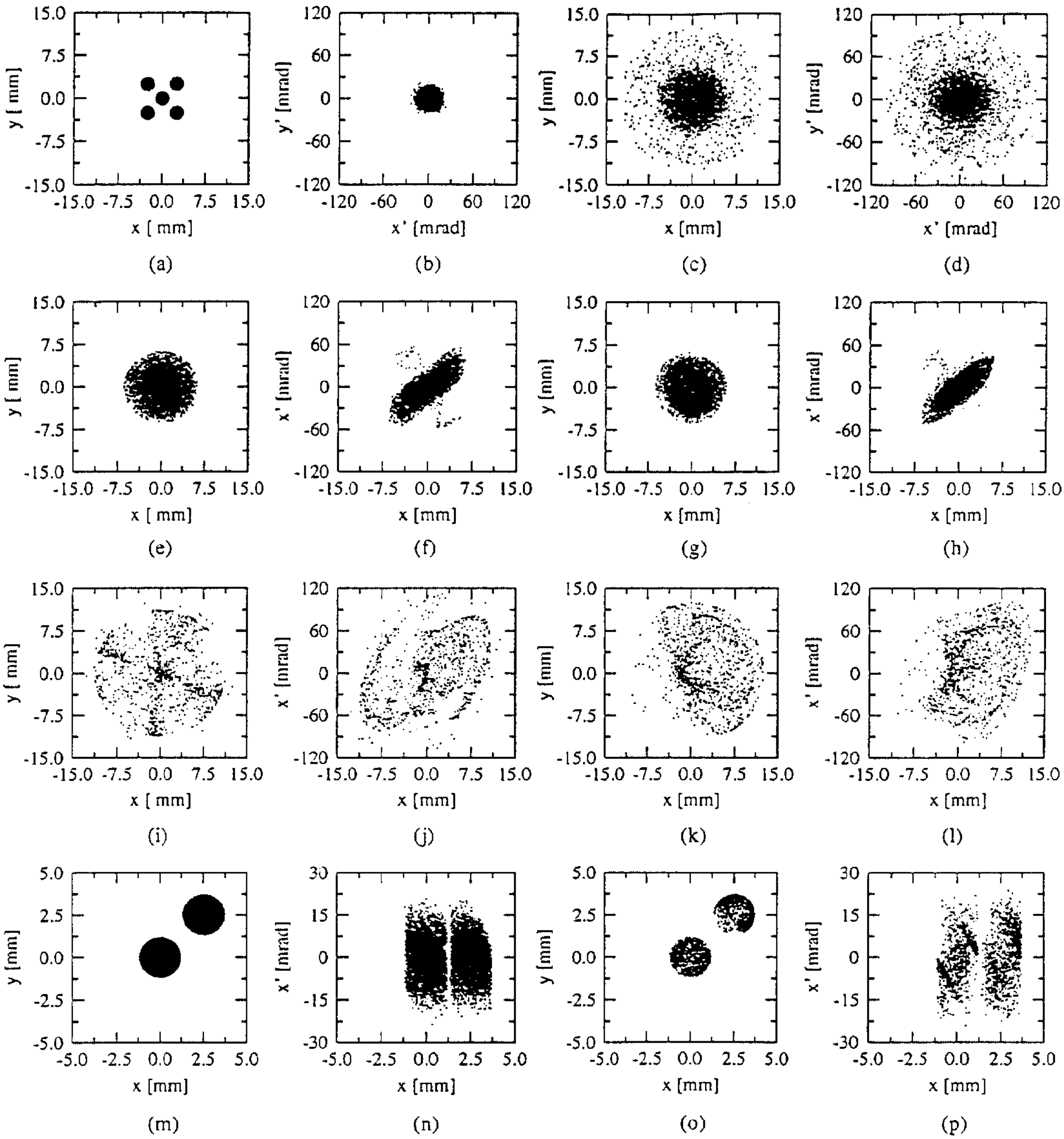

Fig.3. (a) and (b)x-y and x'-y' phase spaces for all particles at z=0 cm (N=-2.25); (c) and (d)x-y and x'-y' phase spaces for all particles at z=524 cm (N=36.3) showing diffuse halo; (e) and (f)x-y and x-x' phase spaces for core particles at N=36.3 that originate in the inner beamlet in Fig. 3a; (g) and (h)x-y and x-x' phase spaces for core particles at N=36.3 that originate in the upper right beamlet in Fig. 3a; (i) and (j)x-y and x-x' phase spaces for halo particles at N=36.3 that originate in the inner beamlet; (k) and (l) x-y and x-x' phase spaces for halo particles at N=36.3 that originate in the upper right beamlet; (m) and (n) x-y and x-x' phase spaces for particles in two beamlets of the initial distribution (z=0 cm, N=-2.25) that will be part of the core at N=36.3; and (o) and (p)x-y and x-x' phase spaces for particles in the two beamlets that will be part of the halo at N=36.3.